

Modelling of the two-state lasing and the turn-on delay in 1.55 μm InAs/InP (113)B quantum dot lasers

K. Veselinov, F. Grillot, A. Bekiarski and S. Loualiche

Abstract: Numerical models based on rate equations are used to study carrier dynamics in the two lowest energy levels of an InAs/InP (113)B quantum dot (QD) system. Two different theories are presented, one based on a cascade-relaxation model and the other using an additional efficient carrier relaxation. The comparison between these two theoretical approaches leads to a qualitative understanding of the origin of the two-state lasing in 1.55 μm InAs/InP (113)B (QD) lasers. In order to investigate the QD laser dynamics, numerical results for the turn-on delay of the double laser emission are also presented and discussed.

1 Introduction

Although optics has proved to be the most practical response to the high traffic rate demand for long-haul transmission, its extension to the metropolitan networks down to the home remains an open challenge. The implementation of optics at transmission rate, where other technical solutions exist, requires cost reduction. As a consequence, semiconductor lasers based on low dimensional heterostructures such as quantum dot (QD) lasers are very promising. Indeed, QDs structures have attracted a lot of attention in the last decade, since they exhibit many interesting and useful properties such as low threshold current, temperature insensitivity, chirpless behaviour and optical feedback resistance [1]. As a result, thanks to QDs lasers, several steps towards cost reduction can be reached such as improving the laser resistance to temperature fluctuation in order to remove temperature control elements (Peltier cooler), or designing a feedback resistant laser for isolator-free transmissions and optics-free module. Most investigations reported in the literature deal with In(Ga)As QDs grown on GaAs substrates [2, 3]. Also numerous theories about carrier dynamics in these structures have been introduced [4, 5]. It is however important to stress that In(Ga)As/GaAs QDs devices do not allow a laser emission above 1.35 μm which is detrimental for optical transmission. In order to reach the standards of long-haul transmissions, 1.55 μm InAs QD lasers on InP substrate have been developed. Recent experimental studies conducted on these devices have shown that a second laser peak appears in the laser spectrum as the injection power increased. The double laser emission is a common property found independently by different research groups for In(Ga)As/GaAs as

well as for InAs/InP systems [6–8]. In order to explain its physical origin, carrier dynamics is at first investigated by comparing two theories: two-state laser competition and the efficient carrier relaxation. Numerical results reporting the double laser emission are then shown exhibiting two different behaviours. The effect of this phenomenon on the turn-on dynamics is also studied. All these recent results will be reviewed later in the Paper.

2 Numerical models

Numerical models based on rate equations are used to study carrier dynamics in the two lowest energy levels of an InAs/InP (113)B QD system. For simplicity, the existence of higher excited states is neglected and a common carrier reservoir is associated to both wetting layer (WL) and barrier. It is assumed that there is only one QD ensemble, that is all dots have the same size meaning that the inhomogeneous broadening of the laser spectrum is not considered. The QDs are assumed to be always neutral and electrons and holes are treated as eh-pairs. It is also important to stress that a single mode laser emission as well as a linear gain variation are assumed in the calculations. Thermal effects and carrier losses in the barrier region are finally not taken into account.

2.1 Two-state lasing competition

Fig. 1a shows a schematic representation of the cascade-relaxation model. First an external carrier injection fills directly the WL reservoir with rate I . Some of the eh-pairs are then captured on the 4-fold degenerate excited state (ES) of the QD ensemble with a capture time τ_{ES}^{WL} and some of them recombine spontaneously with a τ_{ES}^{sp} . Once on the ES, carriers can relax on the 2-fold ground state (GS), be thermally re-emitted in the WL reservoir, recombine spontaneously or by stimulated emission of photons with ES resonance energy. The same dynamic behaviour is followed for the carrier population on the GS level with regard to the ES. This approach has been previously developed for the In(Ga)As/GaAs system [7], but in the case of InAs/InP (113)B system, it is assumed that at low injection rates, the relaxation processes are phonon-assisted, whereas the Auger effect dominates when the injection gets larger

© The Institution of Engineering and Technology 2006

IEE Proceedings online no. 20060043

doi:10.1049/ip-opt:20060043

Paper first received 24th April and in revised form 7th July 2006

K. Veselinov, F. Grillot and S. Loualiche are with the Laboratoire d'Etude des Nanostructures à Semiconducteurs, UMR CNRS FOTON 6082, Institut National des Sciences Appliquées, 20 avenue des buttes de Coesmes, 35043 Rennes Cedex, France

A. Bekiarski is with the Technical University of Sofia, 8, Kliment Ohridski St, Sofia-1000, Bulgaria

E-mail: kiril.veselinov@ens.insa-rennes.fr

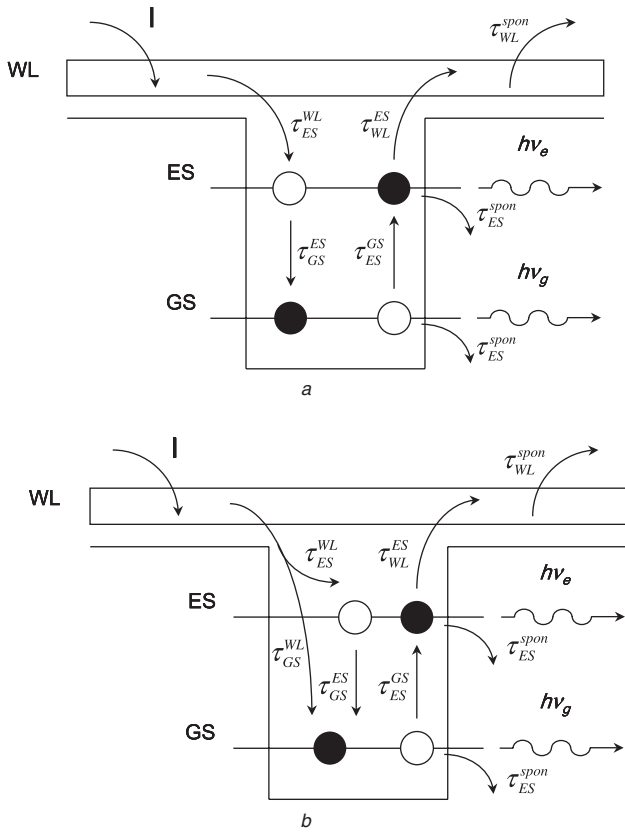


Fig. 1 Schematic representation of the carrier dynamics models
a Intraband energy competition model
b Efficient carrier relaxation model

[9]. The capture and the relaxation times are then calculated through a phenomenological relation depending on the number of eh-pairs in the WL reservoir [10]

$$\tau_{ES}^{WL} = \frac{1}{A_W + C_W N_W} \quad \tau_{GS}^{ES} = \frac{1}{A_E + C_E N_W} \quad (1)$$

where $A_W(A_E)$, $C_W(C_E)$ are the coefficients for phonon and Auger-assisted relaxation respectively, related to the WL and the ES. Their values have been experimentally estimated as follows: $A_W = 1.35 \times 10^{10} \text{ s}^{-1}$, $C_W = 5 \times 10^{-15} \text{ m}^3 \text{ s}^{-1}$, $A_E = 1.5 \times 10^{10} \text{ s}^{-1}$, $C_E = 9 \times 10^{-14} \text{ m}^3 \text{ s}^{-1}$ in a previous work [11].

2.2. Additional efficient carrier relaxation

Part of the work of Veselinov *et al.* [11] reports time-resolved photoluminescence (TRPL) experiments at low temperatures for one InAs QD layer grown by gas-source molecular beam epitaxy on InP (113)B substrate. In order to fit the measured TRPL curves, a direct relaxation channel (τ_{GS}^{WL}) has been introduced to the standard cascade-relaxation model as shown in Fig. 1b. Carriers are either captured from the WL reservoir into the ES or directly into the GS within the same time $\tau_{GS}^{WL} = \tau_{ES}^{WL}$. This assumption has been made after analysis of the kinetic curves in the work of Miska *et al.* [9] where the ES and GS populations gave rise 10 ps after excitation and the time deviation between them has been considered too small. On the other hand, carriers can also relax from the ES to the GS. The other transition mechanisms remain the same as in the previous model. The eh-pairs escape times have been derived considering a Boltzmann

distribution for the ES and GS populations for the system in thermal equilibrium without external excitation

$$\tau_{ES}^{GS} = \frac{1}{2} \tau_{GS}^{ES} \exp\left(\frac{E_{ES} - E_{GS}}{k_B T}\right) \quad (2)$$

$$\tau_{WL}^{ES} = 4 \tau_{ES}^{WL} \exp\left(\frac{E_{WL} - E_{ES}}{k_B T}\right)$$

3 Simulation results and discussion

Following the sketch in Fig. 1a, a five rate equations system (RES) has been analysed, describing the variation of the carrier numbers of the three electronic energy levels and the photon numbers in the cavity with ES and GS resonant energies.

$$\frac{dN_{WL}}{dt} = \frac{I}{e} + \frac{N_{ES}}{\tau_{ES}^{WL}} - \frac{N_{WL}}{\tau_{ES}^{WL}} f_{ES} - \frac{N_{WL}}{\tau_{WL}^{spon}} \quad (3)$$

$$\frac{dN_{ES}}{dt} = \frac{N_{WL}}{\tau_{ES}^{WL}} f_{ES} + \frac{N_{GS}}{\tau_{ES}^{GS}} f_{ES} - \frac{N_{ES}}{\tau_{ES}^{WL}} - \frac{N_{ES}}{\tau_{ES}^{GS}} f_{GS} - \frac{N_{ES}}{\tau_{ES}^{spon}} - N_B \Gamma v_g a_{ES} \left(\frac{N_{ES}}{2N_B} - 1\right) S_{ES} \quad (4)$$

$$\frac{dN_{GS}}{dt} = \frac{N_{ES}}{\tau_{ES}^{GS}} f_{GS} - \frac{N_{GS}}{\tau_{ES}^{GS}} f_{ES} - \frac{N_{GS}}{\tau_{GS}^{spon}} - N_B \Gamma v_g a_{GS} \left(\frac{N_{GS}}{N_B} - 1\right) S_{GS} \quad (5)$$

$$\frac{dS_{ES}}{dt} = N_B \Gamma v_g a_{ES} \left(\frac{N_{ES}}{2N_B} - 1\right) S_{ES} - \frac{S_{ES}}{\tau_p} + \beta_{sp} \frac{N_{ES}}{\tau_{ES}^{spon}} \quad (6)$$

$$\frac{dS_{GS}}{dt} = N_B \Gamma v_g a_{GS} \left(\frac{N_{GS}}{N_B} - 1\right) S_{GS} - \frac{S_{GS}}{\tau_p} + \beta_{sp} \frac{N_{GS}}{\tau_{GS}^{spon}} \quad (7)$$

where $N_{WL,ES,GS}$ are the populations in the WL reservoir, ES and GS and N_B is the total number of QDs. $S_{ES,GS}$ are the photon populations in the cavity with ES and GS resonant energy and $f_{ES,GS}$ are the probabilities to find carrier, assuming 4-fold and 2-fold degenerated ES and GS, respectively.

$$f_{ES} = 1 - \frac{N_{ES}}{4N_B} \quad f_{GS} = 1 - \frac{N_{GS}}{2N_B} \quad (8)$$

The contribution of the ES and GS spontaneous emissions into the lasing mode is denoted by the coefficient β_{sp} and $\tau_p = 1/v_g[\alpha_i + \ln(1/R_1 R_2)/(2L)]$ is the photon lifetime with $v_g = c/n_r$ being the group velocity, n_r the gain material refractive index, α_i the internal loss, R_1 and R_2 the cavity mirror reflectivities and L the laser length. The steady-state solution for the emitted photons is obtained by a numerical calculation of the system for a linear increase of the injection current density. The simulations are made assuming a InAs/InP (113)B laser with six QD stacked layers. The three energy levels in this system are set according to Miska *et al.* [9]. Its cavity length is 2.45 mm and its width is 120 μm . The QD surface density for this system is $5 \times 10^{10} \text{ cm}^{-2}$ and the total number of dots is calculated to be $N_B = 4.41 \times 10^9$. The optical confinement factor is chosen $\Gamma = 0.06$, $\beta_{sp} = 10^{-4}$ and $\alpha_i = 6 \text{ cm}^{-1}$ according to Sugawara *et al.* [12]. The other parameters used for the simulations are as follows: the mirror reflectivities $R_1 = R_2 = 0.3$,

$n_r = 3.27$ for InAs QD and the spontaneous emission times are $\tau_{\text{WL}}^{\text{spon}} = 500$ ps, $\tau_{\text{ES}}^{\text{spon}} = 500$ ps, $\tau_{\text{GS}}^{\text{spon}} = 1200$ ps in agreement with the work of Cornet *et al.* [13]. The steady-state solution is obtained by a numerical calculation of the system for a linear increase of the injection current density. Calculated photon numbers in the cavity are reported in Fig. 2a as a function of the injection current density. Once the threshold of the ES lasing is reached, the emission of the GS saturates and the ES emission increases linearly. This behaviour has been already reported as a two-state lasing competition between the GS and ES due to the finite GS relaxation time for the InAs/GaAs system [4]. However, this approach does not match with recent experimental results obtained on the InAs/InP (113)B [8] system, which have shown no saturation of the GS lasing. On the other hand, a refined second RES has been studied including an effective carrier relaxation model (Fig. 1b) in order to investigate the properties of the InAs/InP (113)B QD device under electrical pumping. This time, the expression $\pm N_{\text{WL}} f_{\text{GS}} / \tau_{\text{GS}}^{\text{WL}}$ has been added to (3) with a minus sign and to (5) with a plus sign in order to include the direct relaxation channel from the WL reservoir to the GS. Simulation of the lasing performance is shown in Fig. 2b where the calculated ES and GS photon numbers are reported as functions of the injection current density. It shows two thresholds corresponding to the two laser emissions. When the ES stimulated emission appears, only a slight decrease of the GS slope efficiency is predicted. At the

same time, the global slope efficiency increases. As a result, simulations show that when a direct relaxation channel is taken into account, the difference between the two threshold currents is doubled. Here, the double laser emission seems to result from the efficient carrier relaxation into the GS due to the increase of the Auger effect for larger injection rates [10]. Although the competition between GS and ES transitions of different QDs is not taken into account, these numerical results give a good qualitative understanding of the experimental results recently reported for an optical pumped InAs/InP (113)B diode laser [8].

The same RES is used to investigate the turn-on dynamics of the InAs/InP (113)B-based diode laser. In Fig. 3, the transient responses of the GS and ES, respectively, are shown for the two models, after introducing a step-like current pulse at time $t = 0$. Its magnitude has been chosen 2.7 times the ES threshold current of the effective carrier-relaxation model (Fig. 2b). In the case of the intraband energy competition (Fig. 3a), the excitation intensity exceeds largely the crossing point of the ES and GS light-current characteristics. Therefore the ES response appears first followed by the GS with time deviation $\Delta t = 88$ ps. The system reaches the steady state after the relaxation oscillations (RO) as fast as $f_{\text{RES}} = 12.8$ GHz for the ES and $f_{\text{RGS}} = 5.2$ GHz for the GS. On the other hand, in the case of the effective carrier-relaxation model, because of the greater threshold current difference and no GS saturation, the system response is inverted and this time the ES characteristic follows the GS one with $\Delta t = 130$ ps. It is shown that the GS trace exhibits a higher RO frequency ($f_{\text{RGS}} = 9.0$ GHz) compared with the ES trace ($f_{\text{RES}} = 4.7$ GHz). In addition, it is important to note that, in this case, the ES intensity modulation is almost two times larger compared with the GS.

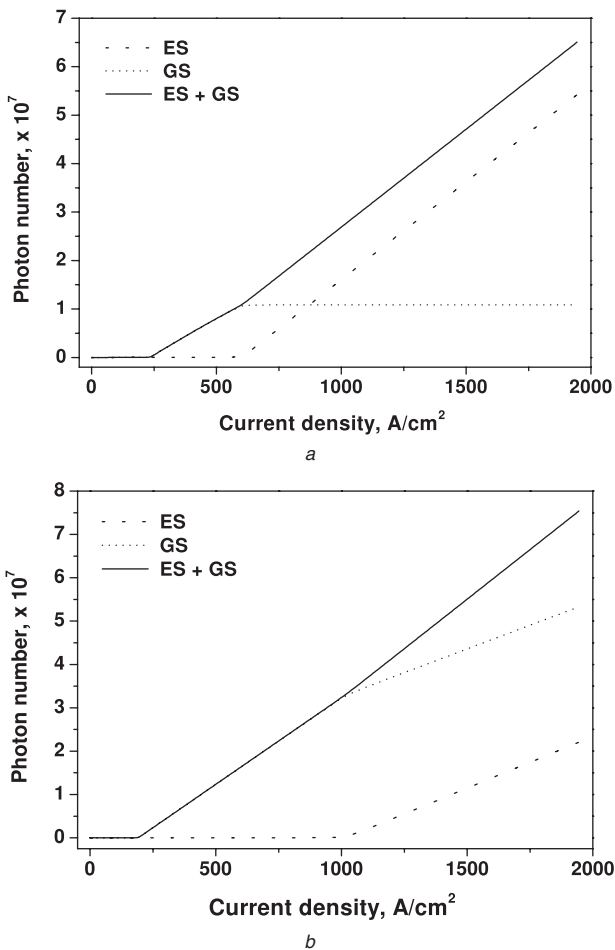


Fig. 2 Calculated photon number in the active region as a function of the injected current density

- a Intraband energy competition model
- b Efficient carrier-relaxation model

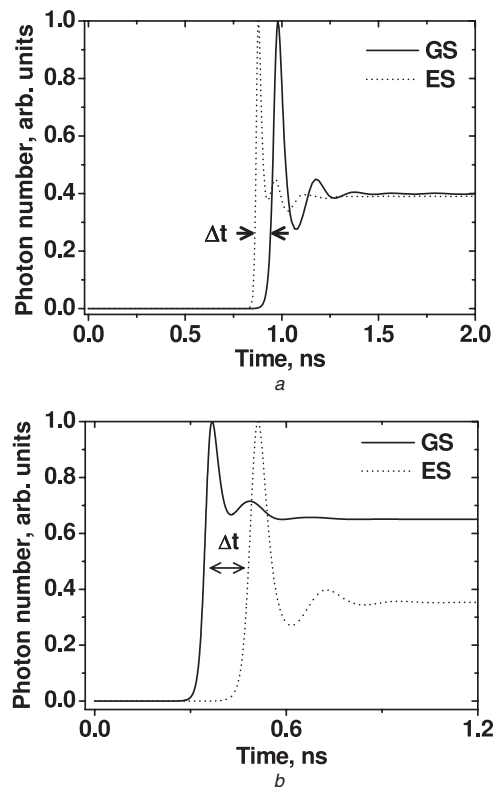


Fig. 3 Turn-on delays for the GS emission (solid line) and for the ES emission (dot line) after a steplike current excitation

- a Intraband energy competition model
- b Efficient carrier-relaxation model

4 Conclusions

In summary, the evolution of photon numbers have been calculated against the injected current density. Using a rate equation model based on the intraband energy competition and on an efficient carrier relaxation, two theoretical approaches have been investigated. On one hand, numerical results describing carrier dynamical behaviour have been presented confirming previously observed phenomena for InAs/GaAs system. On the other hand, it has been shown that the direct relaxation channel included in the model matches very well the different experimental results already published and leads to qualitative understanding of InAs/InP (113)B QD lasers. Also numerical results for the turn-on delay of the double laser emission have been presented exhibiting ROs frequency close to 10 GHz, which is suitable for high-speed transmissions. As a conclusion, a more quantitative analysis with a comparison with experimental results for the double emission from optically pumped QD laser is in preparation. Furthermore, the next step to be done is to improve the numerical model so as to include the effect of the inhomogeneous broadening (QD size dispersion), the nonlinear gain variation and the multimode laser emission as well as to investigate the laser dynamic behaviour under modulation.

5 Acknowledgments

This work was supported by ePIXnet (European Network of Excellence on Photonic Integrated Components and Circuits), SANDiE network of excellence (Self-Assembled semiconductor Nanostructures for new Devices in photonics and Electronics) and CREFID (Centre Régional Francophone d'Ingénierie pour le Développement).

6 References

- 1 Bimberg, D., Grundmann, M., and Ledentsov, N.: 'Quantum dot heterostructures' (John Wiley & Sons, 1999)
- 2 Grundmann, M., Stier, O., BognaÅr, S., Ribbat, C., Heinrichsdorff, F., and Bimberg, D.: 'Optical properties of self-organized quantum dots: modelling and experiments', *Phys. Stat. Sol.*, 2000, **178**, p. 255
- 3 Hatori, H., Sugawara, M., Mukai, K., Nakata, Y., and Ishikawa, H.: 'Room-temperature gain and differential gain characteristics of self-assembled InGaAs/GaAs quantum dots for 1.1–1.3 μm semiconductor laser', *Appl. Phys. Lett.*, 2000, **77**, (6), pp. 773–775
- 4 Mukai, K., Nakata, Y., Otsubo, K., Sugawara, M., Yokoyama, N., and Ishikawa, H.: '1.3- μm CW lasing of InGaAs-GaAs quantum dots at room temperature with a threshold current of 8 mA', *IEEE Photon. Technol. Lett.*, 1999, **11**, p. 1205
- 5 Tan, K.T., Marinelli, C., Thompson, M., Wonfor, A., Silver, M., Sellin, R., Penty, R., White, I., Lammlin, M., Ledentsov, N., Bimberg, D., Zhukov, A., Ustinov, V., and Kovsh, A.: 'High bit rate and elevated temperature data transmission using InGaAs quantum-dot lasers', *IEEE Photon. Technol. Lett.*, 2004, **16**, p. 1415
- 6 Sugawara, M., Hatori, N., Ebe, H., Arakawa, Y., Akiyama, T., Otsubo, K., and Nakata, Y.: 'Modelling room-temperature lasing spectra of 1.3 μm self-assembled InAs/GaAs quantum-dot lasers: homogeneous broadening of optical gain under current injection', *J. Appl. Phys.*, 2005, **97**, p. 043523
- 7 Markus, A., Chen, J.X., Paranthoen, C., Fiore, A., Platz, C., and Gauthier-Lafaye, O.: 'Simultaneous two-state lasing in quantum-dot lasers', *Appl. Phys. Lett.*, 2003, **82**, (12), pp. 1818–1820
- 8 Platz, C., Paranthoen, C., Caroff, P., Bertru, N., Labbe, C., Even, J., Dehaese, O., Folliot, H., Le Corre, A., Loualiche, S., Moreau, G., Simon, J.C., and Ramdane, A.: 'Comparison of InAs quantum dot lasers emitting at 1.55 μm under optical and electrical injection', *Semicond. Sci. Technol.*, 2005, **20**, pp. 459–463
- 9 Miska, P., Paranthoen, C., Even, J., Dehaese, O., Folliot, H., Bertru, N., Loualiche, S., Senes, M., and Marie, X.: 'Optical spectroscopy and modelling of double-cap grown InAs/InP quantum dots with long wavelength emission', *Semicond. Sci. Technol.*, 2002, **17**, L63–L67
- 10 Berg, T., Bischoff, S., Magnusdottir, I., and Mork, J.: 'Ultrafast gain recovery and modulation limitations in self-assembled quantum-dot devices', *IEEE Photon. Technol. Lett.*, 2001, **13**, p. 541
- 11 Veselinov, K., Grillot, F., Miska, P., Homeyer, E., Caroff, P., Platz, C., Even, J., Marie, X., Dehaese, O., Loualiche, S., and Ramdane, A.: 'Carrier dynamics and saturation effect in (311)B InAs/InP quantum dot lasers, optical and quantum electronics', *Optical and Quantum Electronics*, 2006, **38**, (4–6), 369–379
- 12 Sugawara, M., Mukai, K., Nakata, Y., and Ishikawa, H.: 'Effect of homogeneous broadening of optical gain on lasing spectra in self-assembled $\text{In}_x\text{Ga}_{1-x}\text{As}/\text{GaAs}$ quantum dot lasers', *Phys. Rev. B*, 2000, **61**, (11), pp. 7595–7603
- 13 Cornet, C., Labbé, C., Folliot, H., Caroff, P., Levallois, C., Dehaese, O., Even, J., Le Corre, A., and Loualiche, S.: 'Time-resolved pump probe of 1.55 μm InAs/InP quantum dots under high resonant excitation', *Appl. Phys. Lett.*, 2006, **88**, p. 171502